

# AN INTEGRATED APPROACH TO SIMULATE GAS TURBINE SECONDARY AIR SYSTEM

Ali Izadi

Seyed Hossein Madani

Samad Power Ltd., Buckinghamshire, UK

[a.izadi@samad-power.co.uk](mailto:a.izadi@samad-power.co.uk)

[h.madani@samad-power.co.uk](mailto:h.madani@samad-power.co.uk)

Seyed Vahid Hosseini

Mahmoud Chizari

University of Hertfordshire, Hatfield, UK

[v.hosseini@herts.ac.uk](mailto:v.hosseini@herts.ac.uk)

[m.chizari@herts.ac.uk](mailto:m.chizari@herts.ac.uk)

## ABSTRACT

One of the most critical parts of a modern gas turbine that its reliability and performance has a great influence on cycle efficiency is the secondary air system (SAS). Modern systems functions to supply not only cooling airflow for turbine blades and vanes but sealing flow for bearing chambers and turbine segments as well as turbine disks' purge flow in order to eliminate hot gas ingestion. Due to the various interactions between SAS and main gas, consideration of the former is substantially crucial in design and analysis of the whole engine. Geometrical complexities and centrifugal effects of rotating blades and disks, however, make the flow field and heat transfer of the problem so complicated AND too computationally costly to be simulated utilizing full 3-D CFD methods. Therefore, developing 1-D and 0-D tools applying network methods are of great interests.

The present article describes a modular SAS analysis tool that is consisted of a network of elements and nodes. Each flow branch of a whole engine SAS network is substituted with an element and then, various branches (elements) intersect with each other just at their end nodes. These elements which might include some typical components such as labyrinth seals, orifices, stationary/rotating pipes, pre-swirls, and rim-seals, are generally articulated with characteristic curves that are extracted from high fidelity CFD modeling using commercial software such as Flowmaster or ANSYS-CFX. Having these curves, an algorithm is developed to calculate flow parameters at nodes with the aid of iterative methods.

The procedure is based on three main innovative ideas. The first one is related to the network construction by defining a connectivity matrix which could be applied to any arbitrary network such as hydraulic or lubrication networks. In the second one, off-design SAS calculation will be proposed by introducing some SAS elements that their characteristic non-dimensional curves are influenced by their inlet total pressure. The last novelty is the integration of the blades coolant calculation process that incorporates external heat transfer calculation, structural conduction and coolant side modelling with SAS network simulation. Finally, SAS simulation of an industrial gas turbine is presented to illustrate the capabilities of the presented tool in design point and off-design conditions.

## NOMENCLATURE

$C_p$  Specific heat capacity at constant pressure [kJ/kg°C]

$H$	Specific Enthalpy [kJ/kg]
$h_c$	Coolant heat transfer coefficient [W/m <sup>2</sup> K]
$K$	Flow function = $\dot{m}/\Delta p$ , Thermal conductivity
$\dot{m}$	Mass Flow Rate [kg/s]
$N$	Gas turbine rotational speed [rpm]
$P$	Pressure [Pa]
$P_r$	Pressure Ratio = $P_{o, Out}/P_{o, In}$
$\dot{Q}$	Heat Flux [W/m <sup>2</sup> ]
$T$	Temperature [K]
$\eta$	Cooling efficiency
$\varepsilon$	Cooling effectiveness
$\beta$	Non-dimensional coolant mass flow parameter
<b>Subscripts:</b>	
$b$	Blade, vane or metal
$c, cl$	Coolant, Coolant side
$CI/CO$	Coolant Inlet/ Coolant Outlet
$G$	Gas side
<b>Superscripts:</b>	
$\infty$	Reference Temperature to calculate heat flux
$s$	Static property
<b>Abbreviations</b>	
$NDMFP$	Non-dimensional Mass Flow Parameter

## INTRODUCTION

Secondary air is one of the principal systems of modern gas turbines which are operated at high turbine inlet temperature to ensure that turbine blades and vanes are supplied with a sufficient amount of cooling air. It is worth to emphasize that the capability of development of gas path components (compressor, combustion chamber and turbine) has reached a high level, leaving small margins for further developments, has made secondary air systems an area where comparable gains can be achieved [1]. Moreover, gas turbine performance investigations reveal that safety, reliability and performance of a gas turbine are highly related to its SAS design. In this respect and due to the fact that the SAS network influences total pressure and temperature of feeding cooling flow, as it was quantitatively presented in [2], simulation and precise estimate of SAS performance is a critical foundation that guarantees not only accurate cycle analysis but also reliable blade and vanes temperature distribution since the latter is crucial for accurate life assessment.

One of the most cited papers in the simulation of the secondary air system is the article of Kutz and Speer [3] published in Journal of Turbomachinery in 1994 in which they

proposed a network of pipes and chambers to articulate the SAS network besides presenting flow characteristic of various typical elements include seals, orifices, pre-swirl nozzles, rotating holes and tapings. Two years later, Speer and Ebenhoch [4] improved the preceding approach by coupling SAS simulation with blade coolant calculation. They applied a differential 1-D equation derived from momentum conservation for coolant channels considering pipe pressure loss, wall heat transfer and wall rotating effect. Energy and mass conservation equations were also included in nodes of SAS network. In 2001, Foley [5] presented a straightforward technique to quantify the SAS performance using a simple flow network interacted with main gas flow through bleeds and returns. To solve the network, he proposed to iteratively adjust the pressure at the internal nodes until all the mass flow into and out of nodes balance.

As could be seen, some scholars have tried to solve the interaction between cycle performance and SAS codes, considering this fact that the boundary conditions of each code are the output results of the other one. Alexiou and Mathioudakis [1] described the modeling of typical SAS elements in an object-oriented environment (PROOSIS) that allows the creation of different configuration in a simple and flexible manner. Their approach was able to be integrated directly in whole engine cycle performance model.

Some others tried to couple SAS simulation and coolant calculation by matching the characteristic curves of secondary air circuit and the flow function of the blade cooling network to define the working point of the system [6]. As a result, it would be possible to investigate the effects of new design solutions on internal air system and on overall cycle performance [6]. Coupling between 1-D blades and vanes cooling flow codes in Matlab as well as 1-D cavity solver with overall SAS fluid network is another challenging area that covered by [7] and [8].

In other aspects, there are also some publications which tried to integrate various aero-thermo-mechanical analyses of SAS. Supposing it to be vital to consider mutual interaction of SAS fluid flow and its surrounding expansion due to heat transfer [9]. Some researchers employed commercial 1-D fluid flow solver that has a specific library for typical SAS elements to model geometric details of gas turbine internal air system [10]. Some others focused on comparing the numerical correlations derived from the 1-D calculation procedure and 3-D CFD modeling for the rotor-stator cavities pressure loss and heat transfer coefficient [11]. Gallar and his colleagues in Cranfield University published a paper to address the transient and time accurate modeling of SAS which were capable to model transient response of the system in rapid transient scenarios [12]. Zheng and Liu [13] investigated the interaction of the SAS and main gas path in a micro gas turbine utilizing 3D CFD approach. Bozzi and D'angelo investigated numerically and experimentally the effect of secondary air system on the performance of a heavy-duty gas turbine [14].

The main motivation of this paper is to address one of the most challenging areas in overall SAS network simulation which is to define a network that is capable to handle reverse flow situation occurred in off-design conditions. Furthermore, although almost all published methods utilized a single set of

correlation or non-dimensional curves for each element types in various off-design conditions, there might be some branches that their non-dimensional curves depends slightly on inlet total pressure so as it is covered in detail in this paper. In addition, a specific treatment is applied on the blades and vanes coolant calculations in which external heat transfer, structural conduction and coolant side heat transfer are considered in a 0-D manner to accurately capture the effects of heat flux on the coolant mass flow rate. To the author's knowledge, there is not any specific publication at least in the open literature that covers all the above-mentioned aspects in a single integrated calculation procedure.

After this section, general approach for SAS simulation will be described and the network definition of elements and nodes are presented. Two main solvers of SAS code, the Element and Network solver, are explained in detail and then SAS network verification will be presented. Then, both cooling calculation and off-design performance will be covered. Finally, to demonstrate the capability of the developed tool in estimation of the design point as well as off-design conditions, the SAS network of an industrial gas turbine is simulated and results are presented.

## 1 GENERAL SECONDARY AIR SYSTEM SIMULATION

The primary importance of SAS Simulation is related to mass flow balance of various branches in SAS network. In other words, precise estimation of cooling and sealing mass flow and discharge temperature of them in various positions of main gas path has a major role in overall mass flow distribution and ultimately on cycle power and efficiency.

In the current proposed procedure for SAS modeling, each branch of SAS network that has a unique mass flow rate is designated as an "*Element*" and consequently, various elements intersect and interact with each other at "*Nodes*". Therefore, this SAS model includes two main subroutines, Element solver for branch mass flow calculation and Network solver to apply mass and energy conservation equations at each node.

Prior to describe the overall procedure of SAS code, it is necessary to explain the role and function of SAS code in relation to other gas turbine analysis packages. As it can be seen in FIGURE 1, SAS-Coolant Model is connected with two other codes named "Cycle Performance Model" and "FEM Thermal-Clearance Model". The data transferred between these tools are described in TABLE 1.

Furthermore, it should be mentioned that the SAS-Coolant model could be integrated with the cycle performance codes to predict cooling and sealing mass flow rate and produce results as reliable and accurate as those obtained from the high fidelity 3-D CFD tools and by very low computational cost. This is a valuable advantage of this method because the coupling between cycle performance codes and commercial software is a cumbersome task which needs high computational facilities.

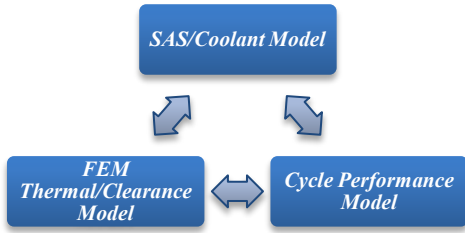


**FIGURE 1: OVERALL CALCULATION PROCESS BETWEEN VARIOUS MODELS**

**TABLE 1: DATA STRUCTURE TRANSFERRED BETWEEN VARIOUS MODELS.**

SAS Input-Output Data	Cycle Performance Model	FEM Thermal-Clearance Model
Input Data (B.C) of SAS-Coolant Model from	Total pressure and temperature at various compressor extraction points and static pressure at the turbine discharge positions.	Total heat flux for each branch, boundary wall temperature and modified clearance for critical positions.
Output Data (results) of SAS-Coolant Model to	Coolant & sealing mass flow and their discharge temperature.	Heat transfer coefficient and averaged flow temperature as $T_{\infty}$

The overall SAS calculation procedure that is illustrated in FIGURE 2 includes four main subroutines. The first subroutine is “SAS\_Read\_InputData” in which the whole data required for simulation is read. The input data include three main categories; (1) Geometric data required for SAS network definition, (2) Cycle and heat transfer boundary conditions (the first row of TABLE 1), and (3) non-dimensional characteristic maps of all elements.

By reading network boundary conditions and creating the SAS network, it could be possible to assign the specified boundary conditions on boundary nodes and then initialize the pressure of internal nodes by boundary pressure (“SAS\_Initialize” subroutine). This initialization is mandatory due to this fact that the calculation procedure is an iterative process and requires the initial value to start. A separate section is devoted to cover initialization process.

The third and the most important subroutine is named “SAS\_Calculation” that contains a “do-while” loop. Before starting this loop, the required maps for some specific elements is interpolated between the provided maps. In short, as it was stated, the maps of rotating elements are provided in various corrected rotor speed and some stationary elements have maps as a function of their inlet total pressure. Therefore, for each set of boundary conditions and prior to start the loop of SAS\_Calculation subroutine, required maps must be generated by the curve interpolation. In SAS\_Calculation subroutine, the first step in do-while loop is to set the nodal data based on their linked elements and as a result, it is possible to implement Element and Network solver subroutines. The exit loop condition is based on evaluation of convergence by analyzing the calculated residuals. Finally, by achieving convergence, the specified results will be available by implementing

“SAS\_Postprocess” subroutine. In the following sections, the most important subroutines will be described in detail.

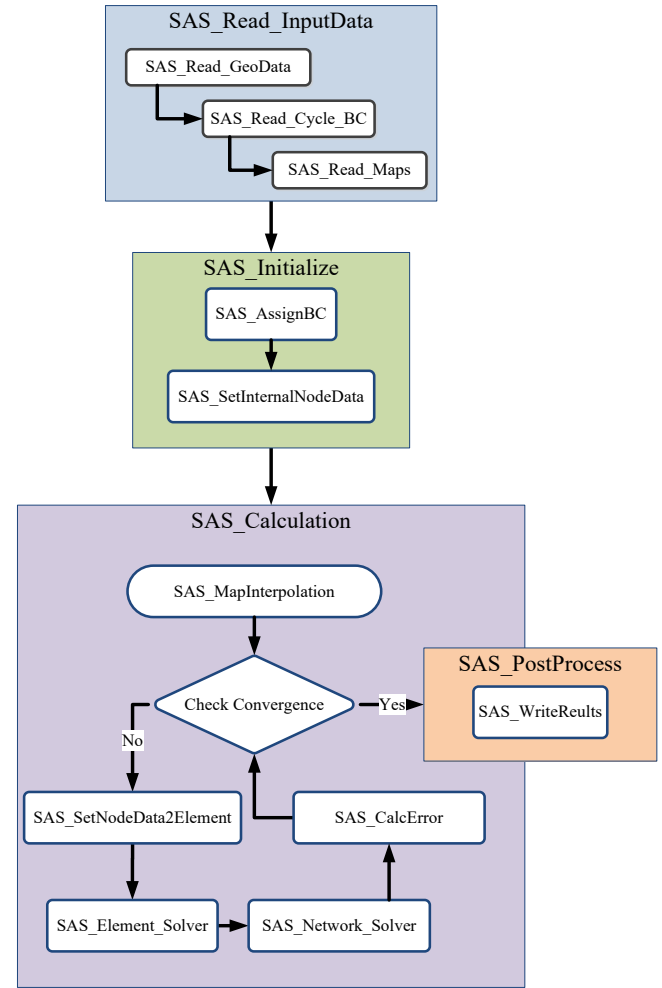


**FIGURE 2: OVERALL SAS CALCULATION PROCEDURE**

## 2 SAS NETWORK DESCRIPTION

Before conducting SAS simulation, overall SAS network including all nodes and elements should be defined in such a way that the connections could be clearly defined. In this respect, a modular structure using object-oriented techniques is considered for SAS network representation that could be easily adjusted for any network configuration. By this method, it is possible to transfer information from nodes to elements and vice versa.

Although this method is utilized here for gas turbine SAS network definition, it is possible to apply it for any other fluid networks such as lubrication systems.

One of the main advantages of this approach is its simplicity of application to generate the system of linear equations required to solve the nodal pressure of SAS network by translating computational domain into network and element matrices. Therefore, prior description of the solution procedure, this network connection specification will be described.

In any arbitrarily configured network, elements are connected to each other at nodes. Inlet elements started with inlet

nodes and outlet ones ends with outlet nodes. Therefore, the simplest network could be a single element network without any internal node and two boundary nodes.

To describe the method clearly, definition of matrices and connections will presented for a sample network which is shown in FIGURE 3.

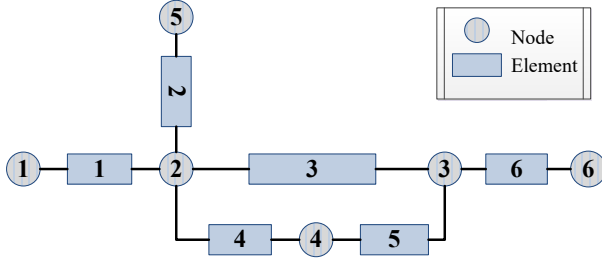


**FIGURE 3:** TYPICAL NETWORK TO DESCRIBE MATRIX DEFINITION

The matrix chain requires the definition of two distinctive matrices: InternalNode and Element2Node. Then the other ones are calculated using these two primary matrices.

*InternalNode Matrix:* There are three different types of nodes: inlet, outlet and internal nodes. All entries of the InternalNode Matrix are zero except ones on the diagonal that are corresponded to the internal nodes. The entries on the diagonal that represent the internal node should be set as unity. In the schematic network depicted in FIGURE 3, only nodes 2, 3 and 4 are internal nodes and therefore, its corresponding matrix is as the one represented in Eq. (1).

$$InternalNode = \begin{bmatrix} 0 & 0 & 0 & 0 & 0 & 0 \\ 0 & 1 & 0 & 0 & 0 & 0 \\ 0 & 0 & 1 & 0 & 0 & 0 \\ 0 & 0 & 0 & 1 & 0 & 0 \\ 0 & 0 & 0 & 0 & 0 & 0 \\ 0 & 0 & 0 & 0 & 0 & 0 \end{bmatrix} \quad (1)$$

*Element2Node Matrix:* The number of rows of this matrix is equal to the network element number and the number of its column is equal to the network node number. The matrix entries are based on the definition presented in TABLE 2. Each array of this matrix is corresponded to a relation between a specific element (row) and node (column). If there is not any connection between those element and node, this array should be set zero. If the node is the inlet or outlet of that element, it must be assigned 1 or -1, respectively. Therefore, prior to set the matrix entries, it is required to define default direction for all element flow. These flow directions should be based on the pressure of boundary nodes. The Element2Node Matrix of the schematic network is presented in Eq. (2).

$$Element2Node = \begin{bmatrix} -1 & +1 & 00 & 00 & 00 & 00 \\ 00 & -1 & 00 & 00 & +1 & 00 \\ 00 & -1 & +1 & 00 & 00 & 00 \\ 00 & -1 & 00 & +1 & 00 & 00 \\ 00 & 00 & +1 & -1 & 00 & 00 \\ 00 & 00 & -1 & 00 & 00 & +1 \end{bmatrix} \quad (2)$$

**TABLE 2:** ELEMENT2NODE DEFINITION

Array	Element-Node Relation
<i>l</i>	The flow direction is from Element to Node; Node is the outlet Node of the Element

<i>-l</i>	The flow direction is from Node to Element; Node is the inlet Node of the Element
<i>0</i>	There is not any connection between them. The node is not connected to the Element.

The InternalNode and Element2Node matrices are derived from the geometry input file. Geometry input file of the schematic network is presented in TABLE 3. As it is indicated in TABLE 3, this file could also include extra information such as inlet and outlet area and radius as well as rotational and returnable conditions of each element. A parameter (Returnable Flag) is also used for branches that have a reversible behavior during the iterations or at some off-design conditions. These elements are provided with extended maps for reverse flow direction.

**TABLE 3:** ELEMENT INPUT DATA OF TYPICAL NETWORK DEPICTED IN FIGURE 3

Element Input Data									
Element Number	Inlet Node	Outlet Node	Element Name	Inlet Area	Outlet Area	Inlet Radius	Outlet Radius	Rotation Flag (0/1)	Returnable Flag (0/1)
1	1	2	Element_1	-	-	-	-	-	-
2	2	5	Element_2	-	-	-	-	-	-
3	2	3	Element_3	-	-	-	-	-	-
4	2	4	Element_4	-	-	-	-	-	-
5	4	3	Element_5	-	-	-	-	-	-
6	3	6	Element_6	-	-	-	-	-	-

*Node2Element Matrix:* This matrix is calculated using the transpose of Element2Node matrix as presented by Eq. (3).

$$Node2Element = -1 * [Element2Node]^T = \begin{bmatrix} +1 & 00 & 00 & 00 & 00 & 00 \\ -1 & +1 & +1 & +1 & 00 & 00 \\ 00 & 00 & -1 & 00 & -1 & +1 \\ 00 & 00 & 00 & -1 & +1 & 00 \\ 00 & -1 & 00 & 00 & 00 & 00 \\ 00 & 00 & 00 & 00 & 00 & -1 \end{bmatrix} \quad (3)$$

*MassFlowCoeff Matrix:* This matrix is evaluated by multiplying InternalNode matrix with Node2Element matrix as Eq. (4).

$$MassFlowCoefficient = InternalNode * Node2Element = \begin{bmatrix} 00 & 00 & 00 & 00 & 00 & 00 \\ -1 & +1 & +1 & +1 & 00 & 00 \\ 00 & 00 & -1 & 00 & -1 & 1 \\ 00 & 00 & 00 & -1 & 1 & 00 \\ 00 & 00 & 00 & 00 & 00 & 00 \\ 00 & 00 & 00 & 00 & 00 & 00 \end{bmatrix} \quad (4)$$

*FlowFunction Matrix:* This is a diagonal, square matrix of order “n” in which “n” equals the number of elements. In this matrix, each diagonal array is equal to the flow function calculated during the solution procedure (Eq. (11)). It is obvious that this matrix will be changed during the iterative solution process and its variation between succeeding iterations will be damped when the solution is converged. Therefore, its variation could be assessed for the convergence evaluation. Exact

definition of flow function and its application in the solution process will be discussed in detail in the Network solver subsection.

$$FlowFunction_i = \begin{bmatrix} K_1 & 0 & 0 & 0 & 0 & 0 \\ 0 & K_2 & 0 & 0 & 0 & 0 \\ 0 & 0 & K_3 & 0 & 0 & 0 \\ 0 & 0 & 0 & K_4 & 0 & 0 \\ 0 & 0 & 0 & 0 & K_5 & 0 \\ 0 & 0 & 0 & 0 & 0 & K_{6-i} \end{bmatrix} \quad (5)$$

*K' Matrix:* This matrix is calculated by multiplying the MassFlowCoeff matrix with FlowFunction matrix (Eq. (6)).

$$K' = MassFlowCoeff * FlowFunction = \begin{bmatrix} 0 & 0 & 0 & 0 & 0 & 0 \\ -K_1 & K_2 & K_3 & K_4 & 0 & 0 \\ 0 & 0 & -K_3 & 0 & -K_5 & K_6 \\ 0 & 0 & 0 & -K_4 & K_5 & 0 \\ 0 & 0 & 0 & 0 & 0 & 0 \\ 0 & 0 & 0 & 0 & 0 & 0 \end{bmatrix} \quad (6)$$

*K'' Matrix:* This matrix is evaluated by Eq. (7).

$$K'' = K' * Element2Node \quad (7)$$

*P0Node Matrix:* This is a vector that contains total pressure of network nodes. The content of this matrix also changes during the solution process.

*Residual Matrix:* This matrix (based on proposed schematic network) defines the system of linear equations of the network and could be calculated as Eq. (8).

$$Residual = K'' * P0Node = \begin{bmatrix} 0 \\ P_1 K_1 - P_2 (K_1 + K_2 + K_3 + K_4) + P_3 K_3 + P_4 K_4 + P_5 K_5 \\ P_2 K_3 - P_3 (K_3 + K_5 + K_6) + P_4 K_5 + P_6 K_6 \\ P_2 K_4 + P_3 K_5 - P_4 (K_4 + K_5) \\ 0 \\ 0 \end{bmatrix} \quad (8)$$

As it will be discussed in Network solver section, each non-zero array of this matrix corresponds to an internal node.

This system of linear equations, which is an expression of the equation of conservation of mass for internal nodes, is solved to obtain the unknown pressure of internal node using element flow functions estimated in the previous iteration.

### 3 INITIALIZATION & NETWORK FLOW DIRECTION

To start the solution iterations, initialization should be carried out for the nodal pressures and temperatures using Eq. (9). In this equation,  $\alpha$  varies between zero and one. For more description, it should be mentioned that each internal node receives its mass flow from a set of possible inlet nodes and it is also a potential source for some set of outlet nodes. The minimum pressure among the all possible inlet nodes (possible sources) is designated as  $P_{0,Inlet,Min}$  and on the other side, the maximum pressure of all possible outlet nodes of that internal node (possible sink) is designated as  $P_{0,Outlet,Max}$ .

$$P_{0,InternalNode} = \alpha(P_{0,Inlet,Min}) + (1 - \alpha)(P_{0,Outlet,Max}) \quad (9)$$

Another important point in this regard is that these initial values should be in compliance with specified flow directions of SAS network and the Element2Node matrix. In other words,

when the overall flow directions of SAS network is specified by Element2Node matrix, initial value of pressure for the element's inlet node should be higher than its outlet node.

As it was discussed by Kutz et al. [3], when a complicated network is analyzed at off-design conditions, or when effects of failures or seal wear are investigated, flow reversal can occur in some of the branches. Furthermore, during the solution iterations, if the calculated pressure of the element's outlet node is higher than its inlet pressure, the element flow direction should be reversed and its reversed map should be used in the next iteration. Some discussion related to symmetric and asymmetric flow elements are covered in the Element solver subsection.

### 4 ELEMENT SOLVER

The main purpose of "Element solver" is to calculate element mass flow rate by interpolation in its characteristic curve in a specific pressure ratio. Indeed, equation of momentum conservation is applied in each element by map interpolation. It is also possible to calculate element mass flow rate using some correlation such as those presented by Kutz [3] and Alexiou [1].

The characteristic non-dimensional mass flow curves are extracted from commercial tools such as Flowmaster in a medium fidelity approach or by ANSYS-Fluent or ANSYS-CFX when the high fidelity approach is preferred. If some wall boundaries of a branch are rotating like the paths around rotor disks, its mass flow is not only dependent on pressure ratio, but the rotational speeds make an important contribution especially in low pressure difference situations. Therefore, there are two distinctive elements in SAS network, stationary and rotating ones. The rotating elements are also divided into two categories based on its flow direction relative to rotor axis. If the element's outlet radius is higher than the element's inlet radius ( $\frac{dr}{dx} = \frac{r_{Outlet} - r_{Inlet}}{x_{Outlet} - x_{Inlet}} > 0$ ), rotational speed has a positive impact on mass flow due to its centrifugal force and increase mass flow rate. On the other side, if the direction of flow is toward to engine axis ( $\frac{dr}{dx} < 0$ ), increasing of rotational speed reduces branch mass flow rate. These effects are depicted clearly in FIGURE 4.

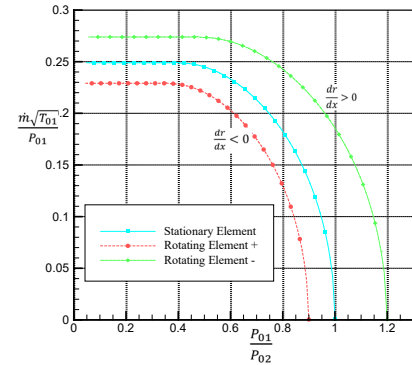


**FIGURE 4:** TYPICAL CHARACTERISTIC CURVES OF NDMFP VERSUS PR

It should be emphasized that some SAS elements such as sudden expansion, T-pieces and nozzles are categorized as the "asymmetric" flow elements. On the contrary, some elements

have symmetrical behavior such as pipes and labyrinth seals. Therefore, the characteristic maps of an asymmetric element is based on their flow directions and for these elements type, two separate maps are required.

As it will be explained in more detail, there are also some elements that those NDMF maps are dependent on their inlet total pressure. For these elements, various maps for some specific inlet total pressure should be supplied.

It should be noted that this proposed SAS model is used in an integrated gas turbine model and its main objective is to provide overall coolant and sealing mass flow rate in design point and various off-design conditions. In this respect, as it is presented in FIGURE 1, SAS model receives its inputs aerodynamic boundary conditions from the cycle gas turbine code and thermal boundary conditions from Thermal-Clearance FEM. To be more precise, it could be emphasized that this SAS model provide heat transfer coefficient and adiabatic wall temperature for the FEM model and received total heat flux of all SAS boundaries from this FEM model.

Indeed, heat transfer calculation in each element is implemented in a simple control volume approach as presented by Eq. (10).

$$\dot{Q} = \dot{m} (h_{0,out} - h_{0,in}) \quad (10)$$

In conclusion, to be sure about satisfying the equation of energy conservation in each branch, coupling between SAS model and Thermal-Clearance FEM model is crucial. As it will be covered in following section, energy conservation at each internal node is also satisfied by Network solver implementation.

However, it is clear that heat transfer levels of internal cooling passages of blades and vanes are considerably higher than the other sections of SAS network. Therefore, a coolant model considering conduction is developed to account for heat flux transferred from main gas to coolant. This model is briefly introduced in another section named ‘‘Airfoil Cooling Calculation’’.

Therefore, based on initial guess of internal pressure and temperature or the updated ones of the last iteration, mass flow rate and outlet temperature of each element were calculated by the Element solver considering the aforementioned points. Then, the ‘‘Flow Function’’ could be established for each element based on Eq. (11).

$$K_i = \frac{\dot{m}_i}{(P_{0,in} - P_{0,out})_i} \quad (11)$$

It should be noted that the FlowFunction matrix (Eq. (5)) which is updated in this step considered constant during the Network Solver implementation.

## 5 NETWORK SOLVER

In the Network Solver subroutine, the mass conservation equations for each internal node is applied using Eq. (12).

$$\sum_{i=1}^n \dot{m}_i = 0 \rightarrow \sum_{i=1}^n K_i (p_{in} - p_{out})_i = 0 \quad (12)$$

Where ‘‘i’’ is the ID of branch or element adjacent to that mentioned internal node and ‘‘n’’ is the overall number of elements that is connected to this node.

Eq. (12) is exactly the compact form of each non-zero arrays of the residual matrix explained in the previous section (Eq. (8)). By solving this residual matrix, the pressure of each internal node will be obtained and then utilized in the following iteration of the Element Solver subroutine. Using this method, which is originally based on the procedure proposed by Meitner [15], mass flow calculations in elements were coupled with the pressure calculation of internal node.

The next step in the Network Solver is the determination of internal temperature by means of energy conservation equation. To do so, it is assumed that all outlet branches of each node have the same temperature. Therefore, the energy equation for nodes is as Eq. (13):

$$\sum_{inlet} \dot{m}_i H_{0i} = \sum_{outlet} \dot{m}_i H_{0i} \rightarrow H_{0,outlet} = \frac{\sum_{inlet} \dot{m}_i H_{0i}}{\sum_{outlet} \dot{m}_i} \quad (13)$$

## 5 NETWORK SOLVER VERIFICATION

To validate the above-mentioned procedure for the SAS network calculation, three different network configurations consisted of three element were checked. The maps of these elements are derived using Flowmaster software that is widely used for the 1-D analysis of the gas turbine SAS network. These maps are implemented in the network code and the results of each configuration were compared with the Flowmaster data. Element Type 1 and 3 are annular pipes that one of their internal or external walls could rotate and Element type 2 is a 3-finned labyrinth seal. The characteristic maps of these elements are illustrated in FIGURE 5.

The generated overall network map by the SAS code for various configurations are compared with the Flowmaster produced network map in FIGURE 6, FIGURE 7 and FIGURE 8. As it can be seen in these figures, the elements of the parallel configuration have a minor effect on each other and behave independently, but in series configurations, the choked mass flow of labyrinth seal dictates overall mass flow of the branch. These figures show that the Network Solver of the SAS code behaves reasonably and produces validated and reliable results.

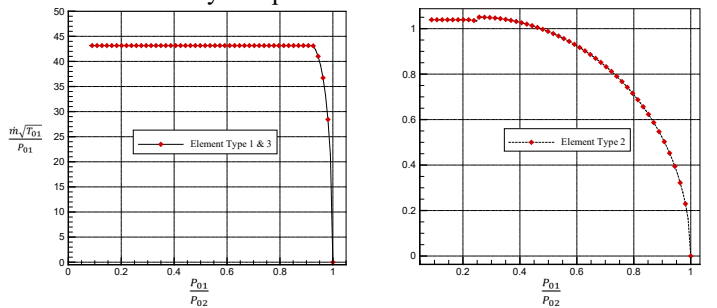
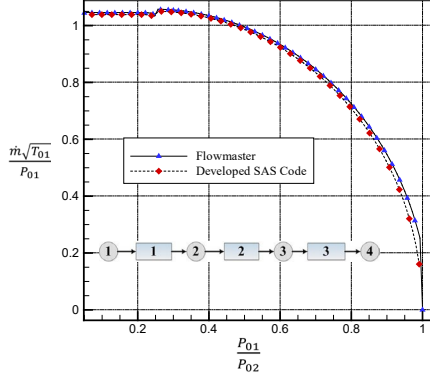
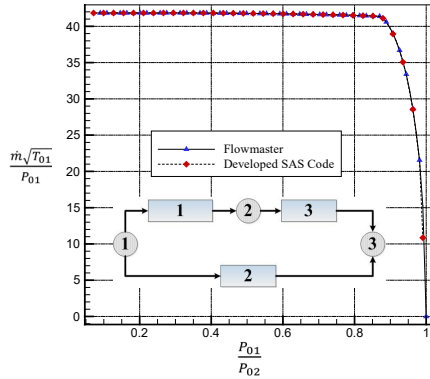


FIGURE 5: NDMFP VS. PR FOR ELEMENT TYPE 1 & 3 (A), ELEMENT TYPE 2 (B)



**FIGURE 6:** COMPARISON BETWEEN RESULTS OF SAS CODE AND FLOWMASTER (SERIES CONFIGURATION)



**FIGURE 7:** COMPARISON BETWEEN THE RESULTS OF SAS CODE AND FLOWMASTER (COMBINED PARALLEL-SERIES CONFIGURATION)

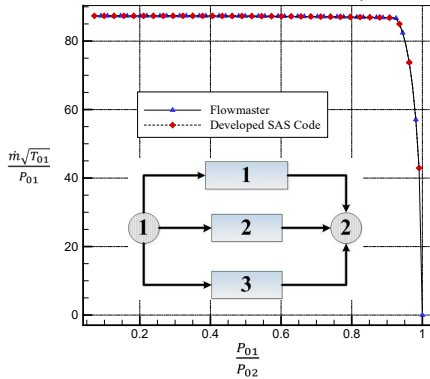


**FIGURE 8:** COMPARISON BETWEEN THE RESULTS OF SAS CODE AND FLOWMASTER (PARALLEL CONFIGURATION)

## 6 AIRFOIL COOLING CALCULATION

The main objective of the coolant subroutine is to calculate the coolant mass flow rate as accurate as possible by considering the most influential parameters such as coolant pressure ratio, total heat flux from the main gas path and centrifugal effects in rotating blades. Extensive numerical investigations on the amount of heat flux from various boundaries in the SAS network revealed that blades and vanes cooling channels received the highest amount of heat flux from their surrounding boundaries. In FIGURE 9, the effect of heat flux on an element mass flow rate is shown.

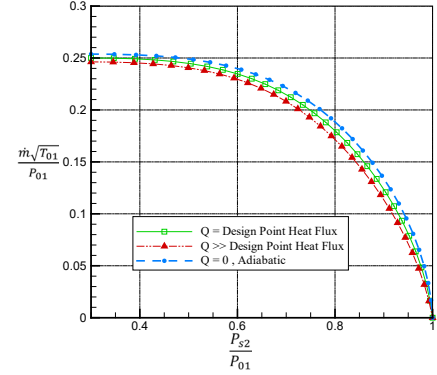


**FIGURE 9:** CORRECTED MASS FLOW RATE FOR AN INTERNALLY COOLED VANE AS A FUNCTION OF OVERALL HEAT FLUX FROM MAIN GAS

Before presenting calculation procedure, some of most important non-dimensional parameters involved in coolant calculation are briefly described.

Among this parameters,  $Re$  and  $Nu$  are used to calculate heat transfer coefficient in the blade gas side and the other ones ( $\epsilon$ ,  $\eta$  and  $\beta$ ) are used for coolant side calculations. Hot gas coming out from the combustion chamber has considerably high temperature and high velocity and its heat transfer coefficient could be roughly estimated using flat plate correlation and then calibrated by CFD. Averaged gas side heat transfer coefficient is estimated by Eq. (14), where  $\alpha$  is 0.37,  $\beta$  is 0.333 and  $m$  is depended on the blade geometry.

$$St = K \cdot Re^\alpha \cdot Pr_g^\beta \left( \frac{T_w}{T_\infty} \right)^m \quad (14)$$

$$h_g = St_g \times Cp_g \times \rho_g \times U_g$$

A simple conduction calculation is implemented to relate gas side and coolant side heat transfer parameters. In this respect, some geometrical data such as gas and coolant side wetted area for heat flux calculation, equivalent blade thickness, TBC thickness and also some thermo-physical properties such as thermal conductivities of blade and TBC are required. In a simple manner and as a result of Fourier's law of heat conduction, a linear temperature distribution is assumed between coolant and gas side. Therefore, averaged and blade temperature could be calculated by Eq. (15).

$$\bar{T}_{Blade} = \frac{\bar{T}_{Gas Side} + \bar{T}_{Coolant Side}}{2} \quad (15)$$

The fundamental equations for blade cooling were presented for the first time by Hoolland and Thawke [14]. The cooling effectiveness ( $\epsilon$ ) was defined by Eq. (16). Although this definition is global and could be used for both internal and film cooled blade, the present method is more suitable for internal blade cooling. To clarify this issue, it should be emphasized that for film cooling calculation, some more sophisticated manipulation is required especially in the total coolant mass flow calculation.

$$\epsilon = \frac{T_g - T_b}{T_g - T_{cl,in}} \quad (16)$$

Further, cooling efficiency ( $\eta_c$ ) was defined as the ratio of the actual temperature rise to the maximum possible rise [15]:

$$\eta_c = \frac{T_{cl,out} - T_{cl,in}}{T_b - T_{cl,in}} \quad (17)$$

The non-dimensional coolant mass flow parameter or the heat capacity ratio is defined as:

$$\beta = \frac{\dot{m}_{cl} C_{p,cl}}{h_g A_g} = \frac{T_g - T_b}{T_{cl,out} - T_{cl,in}} \quad (18)$$

Cooling effectiveness could also be derived as a function of non-dimensional coolant mass flow parameter using CFD simulation. FIGURE 10 shows CFD results of the cooling effectiveness versus the non-dimensional coolant mass flow parameter and the fitted curve for the first stage vane of a typical industrial gas turbine.

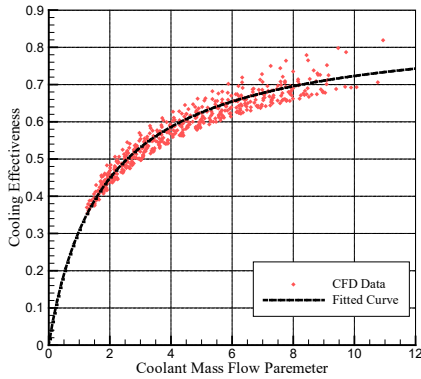


**FIGURE 10: COOLING EFFECTIVENESS VS. NON-DIMENSIONAL COOLANT MASS FLOW FOR THE FIRST STAGE VANE OF A TYPICAL INDUSTRIAL GAS TURBINE**

In FIGURE 11, the cooling calculation procedure is illustrated. As shown, this procedure, which is an iterative process, is started by guessing an averaged value for the blade gas side temperature. Then by having the gas side flow parameters (such as  $Re$ ,  $Pr$  and  $T_\infty$ ) obtained from the cycle performance code, heat transferred coefficient and therefore, total heat flux could be estimated using Eq. (14). The next step is to solve blade conduction and calculate the area averaged temperature at the coolant side from the Fourier’s law of heat conduction. Then, the averaged blade temperature is possible to estimate by Eq. (15).

In coolant side, only two governing equations are applied that originated from momentum and energy conservation equations. At first, knowing both the total heat flux exerted to coolant and coolant overall pressure ratio, the coolant non-dimensional mass flow could be interpolated from a plot such as the one shown in FIGURE 9. The total flux is equal to total heat extracted from hot gas path minus the heat flux transferred to disk through the blade root.

It should be emphasized that for rotating blades, the coolant non-dimensional mass flow is also a function of corrected rotating speed. These maps could be derived experimentally or from a coupled-conjugate heat transfer calculation such as the one described in ref. [2].

Secondly, by knowing coolant mass flow and total heat flux, one may calculate coolant outlet temperature and non-

dimensional coolant mass flow parameter using Eq. (10) and Eq. (18), respectively.

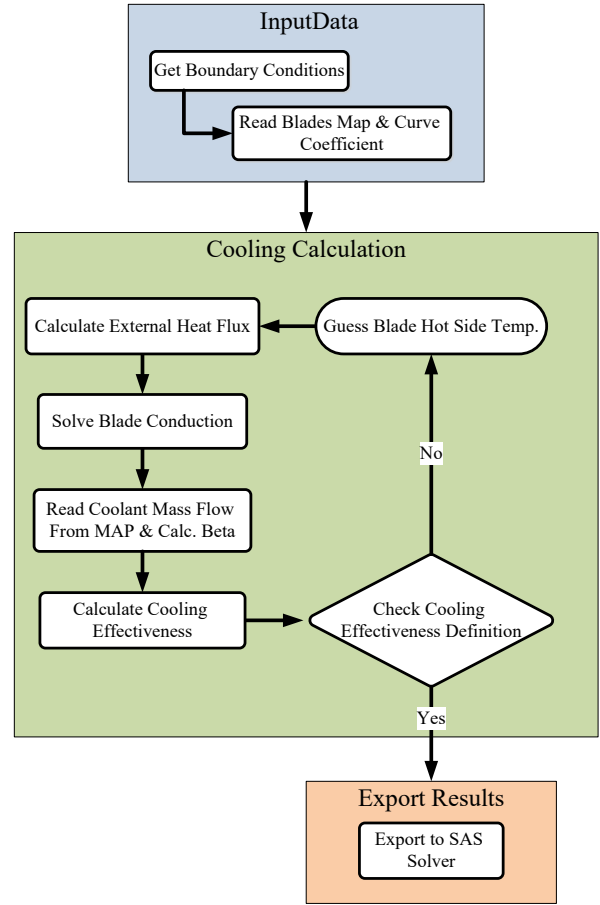


**FIGURE 11: COOLING CALCULATION PROCEDURE**

The cooling effectiveness then could be interpolated from a specific curve like the one presented in FIGURE 10. The final step is to check if the calculated averaged blade temperature and the blade cooling effectiveness is compatible with the effectiveness definition of Eq. (17). In this respect, if these are not compatible with each other, the initial guess for the blade’s gas side temperature is adjusted to fulfill this compatibility equation.

To show the coolant calculation accuracy and its capability in estimating averaged blade temperature, the results of above-mentioned approach is compared with the coupled conjugate CFD results in FIGURE 12, which reveals a small deviation around 4.5 degrees Celsius which is in the worst case below 0.8% and more than sufficient for this purpose.

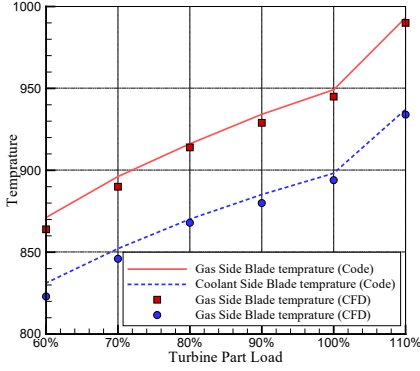


**FIGURE 12: COMPARISON BETWEEN COOLANT CALCULATION PROCEDURE AND CFD RESULTS**

## 6 RESIDUAL CALCULATION AND CONVERGENCE

Among various variables encountered during the calculation process, total pressure of internal nodes and element's mass flow rate are selected for error estimation due to this fact that one of them is updated by the Element solver and the other one is updated by the Network solver.

Root mean squared error for pressure and mass flow rate are derived from Eq. (19) and Eq.(20).

$$\frac{1}{Nn} \sqrt{\sum_{i=1}^{Nn} (P_i^{j+1} - P_i^j)^2} \quad (19)$$

$$\frac{1}{Ne} \sqrt{\sum_{i=1}^{Ne} (\dot{m}_i^{j+1} - \dot{m}_i^j)^2} \quad (20)$$

Convergence criteria ensure that convergence cannot be accidentally reached if the residuals undergo oscillations between two consecutive iterations [9]. If all convergence criteria are fulfilled, the solution is assumed to be converged and the iterative process stops. These criteria include:

- 1- Enough iteration must be carried out. In practice, at least 5 percent of total maximum iteration (100 Iterations) is required for a converged solution.
- 2- The overall trend of calculated error for both variables should be descending.
- 3- In descending trend for each error, at least 8-order of magnitude reduction is required.

The variation of root mean squared error for node's pressure and element's mass flow during the overall iteration process are depicted in FIGURE 13. It is obvious from these plots that both types of root mean squared errors are reduced by several orders of magnitude and as an indication of the solver robustness, the residuals reduced sharply without any oscillation.

## 7 OFF-DESIGN CALCULATION

There might be some SAS stationary paths or branches that their non-dimensional mass flow rate is a slight function of its inlet total pressure. Based on the CFD results, it has been confirmed that if the passage or branch does not include any

orifice or any other type of restriction, its characteristic curve might be sensitive to its inlet total pressure. For example, as it can be seen in FIGURE 14, there is a slight dependency on the inlet total pressure for a typical SAS branch existed in the SAS network of an industrial gas turbine.

Therefore, additional step should be implemented before Element Solver subroutine in off-design calculation. In this respect, after implementation the Network Solver subroutine and when total pressure of all internal nodes are updated, it is required to calculate (by map interpolation) the non-dimensional mass flow curves of these sensitive elements. This new map that is corresponded to the updated inlet total pressure must be utilized in the next Element solver subroutine calculation.

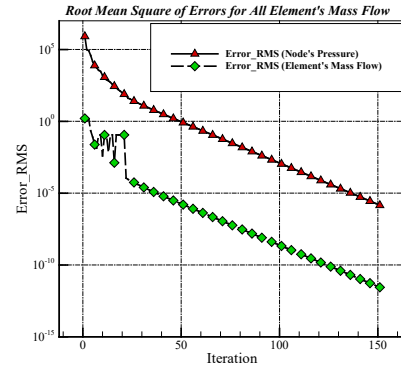


**FIGURE 13: CONVERGENCE HISTORY FOR NODE'S PRESSURE AND ELEMENT'S MASS FLOW**

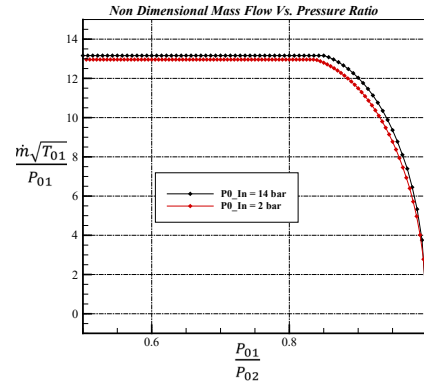


**FIGURE 14: NON-DIMENSIONAL MASS FLOW VS. PRESSURE RATIO FOR ELEMENT SENSITIVE TO ITS INLET TOTAL PRESSURE (ELEMENT # 13)**

## 8 OFF-DESIGN CALCULATION VERIFICATION

The first step for off-design verification is to choose an appropriate path whose non-dimensional mass flow rate is a slight function of inlet total pressure. To do so, a branch with this feature has been chosen to apply dynamic boundary condition to its inlet and outlet nodes. Transient response of this dynamic boundary condition derived from Flowmaster V7 is compared with steady state off-design results of SAS code and is presented in FIGURE 15.

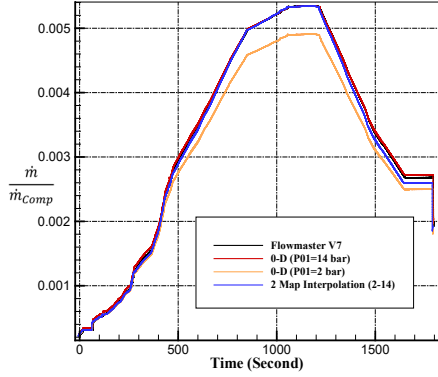


**FIGURE 15: OFF-DESIGN MODEL VERIFICATION**

As it can be seen, the results derived from SAS off-design code supported by a map of two curves for each element is more coincident than the single curve map. It is obvious that at the starting phase and where inlet total pressure is low, the effect of curve corresponded to inlet total pressure of 2 bar is more effective than the curve of 14 bar. On the other hand, near the design point, the curve with 14 bar is used. Therefore, utilizing a two-curve map and map interpolation for each boundary condition resulted in more accurate off-design capability as shown in FIGURE 15.

## 9 CASE STUDY

In last sections, it was shown that the presented model is capable to estimate the mass flow distribution of various configuration of a SAS network in comparison with FlowMaster software. One solution to directly investigate the validation of the SAS model is the measurement of both network boundary condition and mass flow of each channel which requires a customized test rig featured with many test point measurements. But the other solution is to integrate the SAS model with a cycle performance code, then the overall parameters of the engine, which are affected by the SAS mass flow, could be validated against performance test results.

To verify the integrated model, experimental data extracted from performance tests of a number of Siemens SGT-600 engines are used. These tests are performed at various ambient temperatures at the test stand of Rey, Tehran. The solution algorithm in integration of the SAS model and cycle performance code is out of the scope of this paper and will be published by the authors in a separate paper. Maximum relative error for each parameter is less than 1 percent as listed in Table 4 which is acceptable for the SAS model.

In the following, secondary air system of this industrial gas turbine is utilized to show capabilities of the proposed SAS modeling procedure. This SAS network includes some of the common SAS elements such as labyrinth seals, pre-swirl, rotor-stator cavity, disk flow and blade cooling. As it is illustrated in FIGURE 16, the SAS network (colorful paths) includes various branches that extract pressurized gas from various locations of the compressor and discharge them in various points of high and low pressure turbines.

**Table 4: Maximum relative error between experimental and model results**

Parameter	Max. Relative Error (%)
Power	0.8
Turbine Exit Temperature (TET)	0.4
Compressor Pressure Ratio	0.2
Gas Generator Speed	0.4

Compressor casing of the selected gas turbine has two cavities, named LP and HP cavity, downstream of the 2nd and 5th compressor stage, respectively. There is also another extraction at the end of compressor downstream of the last stage rotor at the hub and some other extraction points in the compressor diffuser.

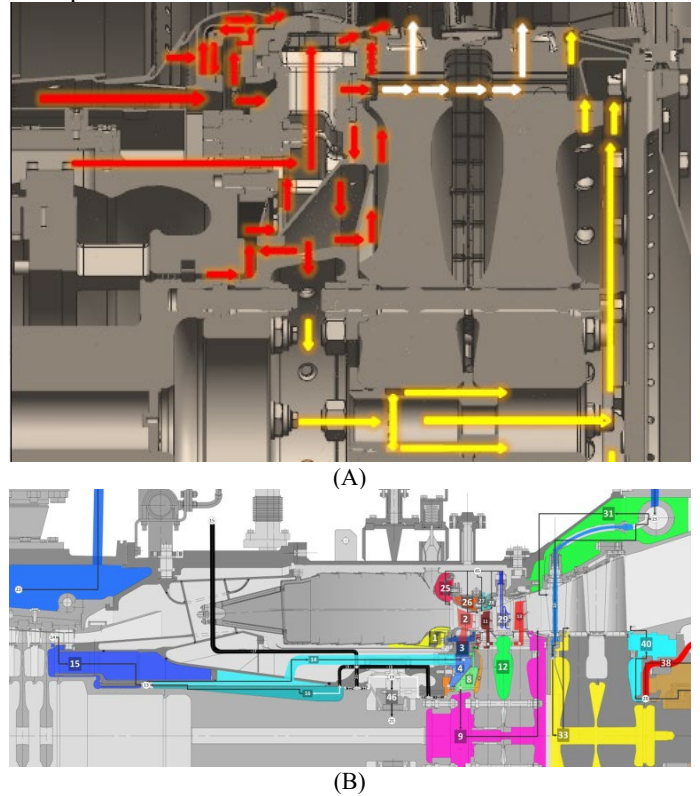


**FIGURE 16: SAS NETWORK AROUND THE ROTOR (A), SCHEMATIC VIEW OF ELEMENTS AND NODES OF SAS NETWORK (B)**

The chosen case study is a twin shaft industrial gas turbine with GG and PT nominal shaft speed about 9800 and 7200 RPM, respectively. Therefore it has four bearings that only one of them is located in the high pressure domain and the other ones are low pressure bearings. To properly seal these low pressure bearing chambers, pressurized gas of LP cavity is utilized. For high pressure bearing chamber, the pressurized gas of compressor diffuser is utilized. This extracted flow has high temperature and therefore, is not suitable to seal bearing and should be cooled in a level below oil degradation limit. Therefore, some equipment is designed that is referred as “Seal Air Cooler”.

Extracted flow from the compressor HP cavity is utilized for the power turbine casing cooling and the only cooled vane of it.

This flow is then conducted to cool the power turbine rotor and seal the rotor-stator cavity of the power turbine first stage.

Required coolant mass flow for the HP turbine casing, rotor and all its cooled vanes and blades are extracted from the compressor diffuser and bypassed from the combustion chambers. A portion of this bypassed flow is conducted through an annulus to feed the sealing requirement of the HP turbine casing and provide the coolant flow for its second stage vane.

As it can be seen in FIGURE 16, one of the most important and complex branch of SAS network is around the HP turbine rotor that is designed to be overwhelmed in the SAS flow. Furthermore, a portion of bypassed flow from the combustion chamber is used for the first vane cooling and its remainder conducted to the pre-swirl nozzle to make the flow appropriate to be entered into the first and second blade cooling ports.

The characteristic curves of some of the stationary and rotating elements of this proposed network are shown in FIGURE 17 and FIGURE 18.

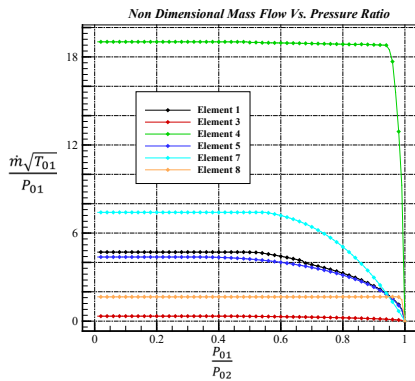


FIGURE 17: NON-DIMENSIONAL MASS FLOW VS. PRESSURE RATIO, STATIONARY ELEMENTS

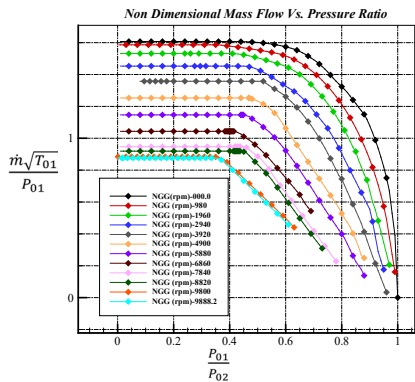


FIGURE 18: NON-DIMENSIONAL MASS FLOW VS. PRESSURE RATIO, ROTATING ELEMENT, ELEMENT#9

## RESULTS AND DISCUSSIONS

Prior to describe the trend and quality of results, some explanations regarded to SAS boundary conditions and location is provided. Locations of inlet and outlet boundary nodes for described SAS case study are depicted in FIGURE 19.

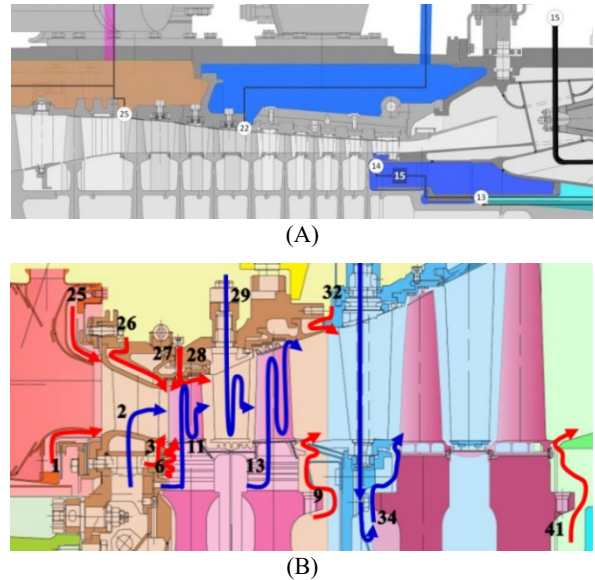


FIGURE 19: LOCATION OF SAS INLET (A), AND OUTLET BOUNDARY CONDITIONS (B)

In order to illustrate off-design as well as design point performance of SAS code and its capability to produce reliable and robust results, the typical mission of normal start-normal shutdown is selected and the corresponding boundary conditions in this mission is applied. For inlet node both total pressure and temperature are applied while for the outlet nodes only static pressure is applied. These boundary conditions for inlet and outlet nodes are illustrated in FIGURE 20 and FIGURE 21.

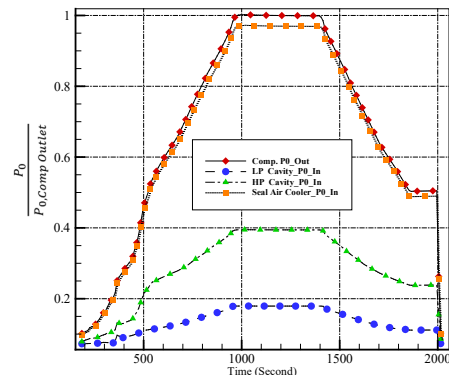
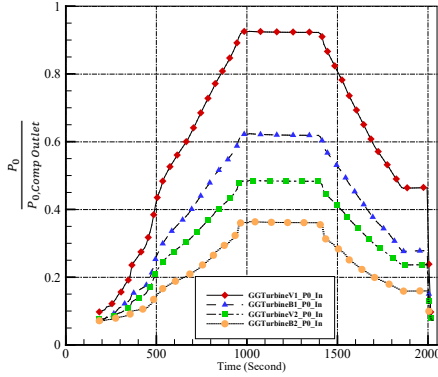


FIGURE 20: APPLIED BOUNDARY CONDITIONS (TOTAL PRESSURE) TO SAS INLET BOUNDARIES

Mass flow percentage for various cooling and sealing purposes in design point condition is illustrated in FIGURE 22. It is also found that overall blades and vanes cooling accounts for approximately 60% of the total SAS mass flow that is reasonable for this typical SAS design and consistent with existing rules of thumb.

It should also be emphasized that almost 90% of the total SAS mass flow extracted from the compressor outlet and utilized for the HP turbine cooling and its gas path sealing.



**FIGURE 21:** OUTLET STATIC PRESSURE IN NORMAL START-NORMAL SHUTDOWN MISSION APPLIED AS B.C. TO SAS OUTLET BOUNDARIES

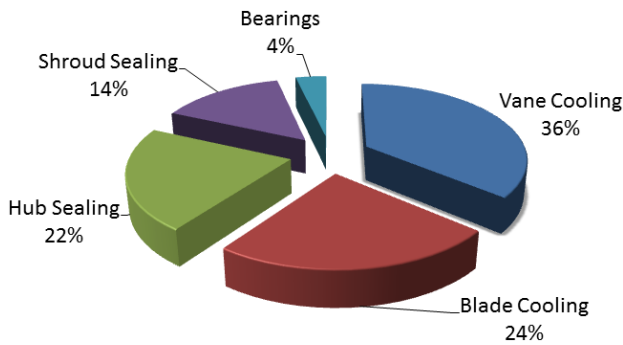


**FIGURE 22:** COOLING & SEALING MASS FLOW DISTRIBUTION AT DESIGN POINT CONDITION

As it is presented in the next figures, it could be concluded that the SAS flow distribution and its corresponding percentage for each discharge position would be assumed constant in the almost entire off-design situations from the starting of loading to the 100% base load. Extracted mass flow rate in inlet nodes as well as discharge mass flow at the exit paths in various off-design conditions are depicted in FIGURE 23, FIGURE 24 and FIGURE 25. It should be mentioned that all values presented through FIGURE 20 to FIGURE 25 are non-dimensionalized by their corresponding values of the compressor outlet. As it is illustrated in FIGURE 24, the highest cooling mass flow is related to the blades and vanes of the HP turbine's first stage.

It is also concluded from FIGURE 25 that the highest sealing mass flow is related to the Path 1 and Path 25. These mass flows are utilized to more dilute the outgoing combustion chamber gas flow, to protect the hub and shroud of the first stage vanes from the hot gas and finally to adjust TIT.

Secondary air system analysis by the network of elements and nodes approach neither requires a large amount of computing resources nor a large amount calculation time. For the presented model that includes 46 elements and 46 nodes, by applying the above-mentioned convergence criteria, the convergence reaches after a total 150 iterations. This corresponds to roughly 2.63 second on the Intel(R) Core(TM) i7 @ 4.0 GHz machine.

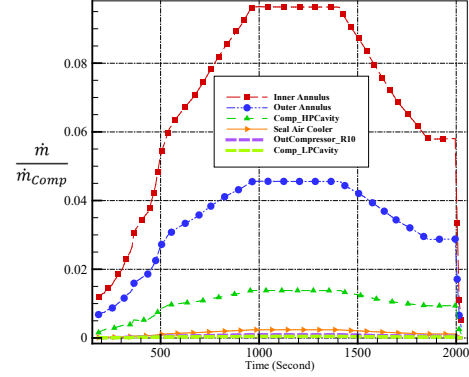


**FIGURE 23:** EXTRACTED MASS FLOW RATE IN VARIOUS POSITION OF COMPRESSOR IN NORMAL START-NORMAL SHUTDOWN MISSION

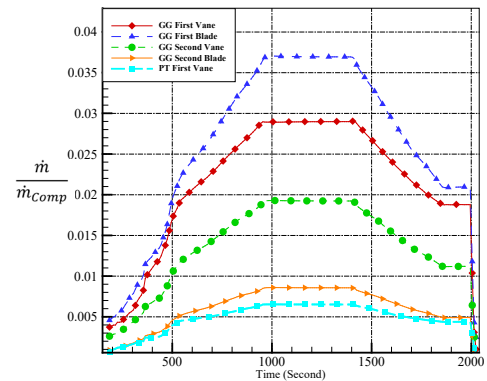


**FIGURE 24:** CALCULATED COOLING MASS FLOW RATE IN NORMAL START-NORMAL SHUTDOWN MISSION

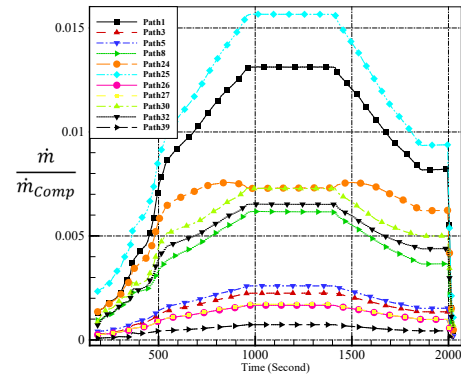


**FIGURE 25:** CALCULATED SEALING MASS FLOW RATE IN NORMAL START-NORMAL SHUTDOWN MISSION

## CONCLUSION

The work rendered herein covers the development of a robust 0-D map based procedure for SAS calculation including blades and vanes cooling estimation.

The presented procedure for SAS calculation guarantees accurate mass flow distribution in various SAS branches at near real time frame rate and at low computational cost, if element's non-dimensional maps are reliable and accurate. In other words, it is possible to extract non-dimensional maps of various branches of SAS network by a high fidelity, high computational

approaches using full 3D CFD models and implement them into a low-fidelity model (SAS code).

Results of sealing and cooling mass flow during a typical mission revealed that almost all discharge mass flow obey a rather unique behavior that is related to the implemented boundary condition. In other words, each discharge mass flow could be estimated by a specific and constant fraction of the engine mass flow at off-design conditions.

At the light of previous discussion, it will be also worthy to mention that the bearing chamber boundary condition would have a great influence on the SAS mass flow distribution, if it is located on the high pressure region. As a consequent, it is so vital to couple SAS network modeling and the lubrication system simulation to exactly calculate required sealing mass flow for high pressure bearing. Indeed, if the estimated bearing chamber pressure is so low, it behaves like a sink and extracts lots of SAS mass flow. On the other hand, if it is overestimated, it might lead to a situation in which the oil leaks to the SAS network and causes it to be burned.

In addition, the proposed method has such flexibility that its Element solver could utilize various experimental correlations instead of element's maps for element mass flow calculations.

Furthermore, it should emphasize that there are multitude potentials for accuracy improvements such as:

- 1- Development a library for heat transfer coefficient of various elements of SAS network.
- 2- Develop the module responsible for windage effect.
- 3- Develop a procedure to increase the accuracy of calculated blade's and vane's heat flux at the gas side by considering combustion radiation.
- 4- Substitution the maps of the coolant mass flow by a 1-D cooling method such as the one presented by ref. [2].

Finally, it is worthy to emphasize that in an early design phase, this method is a suitable tool for optimizing cooling and secondary air system or even it is a valuable tool for upgrading cycle design point through minimizing cooling and sealing mass flow.

## ACKNOWLEDGMENTS

The authors would like to express their appreciation to TurboTec Company, especially H. Khaledi and M. Samani for their support in providing geometry and operating data of the typical gas turbine.

## REFERENCE

- [1] A. Alexiou and K. Mathioudakis, "Secondary Air System Component Modeling for Engine Performance Simulations," *Journal of Engineering for Gas Turbines and Power*, vol. 131, pp. 031202-1, 031202-9, May 2009.
- [2] M. Alizadeh, A. Izadi and M. Fathi, "Sensitivity Analysis on Turbine Blade Temperature Distribution Using Conjugate Heat Transfer Simulation," *J. Turbomach*, vol. 136, 2013.
- [3] K. J. Kutz and T. M. Speer, "Simulation of the Secondary Air System of Aero Engines," *J. Turbomach*, vol. 116, pp. 306-315, 1994.
- [4] G. Ebenhoch and T. M. Speer, "Simulation of Cooling Systems in Gas Turbines," *J. Turbomach*, vol. 118, pp. 301-306, 1996.
- [5] A. Foley, "On the Performance of Gas Turbine Secondary Air System," in *ASME Turbo Expo*, New Orleans, 2001.
- [6] L. Bozzi, S. Traverso, C. Carcasci, B. Facchini and S. Gori, "Heavy Duty Gas Turbine Simulation: Global Performances Estimation and Secondary Air System Modifications," in *ASME Turbo Expo*, Barcelona, 2006.
- [7] M. Cerutti, L. Bozzi and C. Carcasci, "An Efficient Procedure for the Analysis of Heavy Duty Gas Turbine Secondary Flows In Different Operating Conditions," in *ASME Turbo Expo*, Glasgow, 2010.
- [8] F. Bonzani, L. Bozzi, M. Mantero and A. Vinci, "1D Tool for Stator-Rotor Cavities Integrated Into A Fluid Network Solver of Heavy-Duty Gas Turbine Secondary Air System," in *ASME Turbo Expo*, Glasgow, 2010.
- [9] Y. Muller, "Secondary Air System Model for Integrated Thermomechanical Analysis of a Jet Engine," in *ASME Turbo Expo*, Berlin, 2008.
- [10] F. K. Benra, H. J. Dohmen and O. Schneider, "Application of an Enhanced 1D Network Model To Calculate The Flow Properties of A Pre-Swirl Secondary Air System," in *ASME Turbo Expo*, Berlin, 2008.
- [11] C. Bianchini, R. Da Soghe, B. Facchini, L. Innocenti, L. Bozzi, S. Traverso and M. Miccio, "Development of Numerical Tools for Stator-Rotor Cavities Calculation In Heavy-Duty Gas Turbines," in *ASME Turbo Expo*, Berlin, 2008.
- [12] L. Gallar, C. Calcagni, C. Liorens and V. Pachidis, "Time accurate modelling of the secondary air system response to rapid transients," *Proceedings of the Institution of Mechanical Engineers, Part G: Journal of Aerospace Engineering*, vol. 225, no. 8, p. 946-958, 2011.
- [13] Y. Zeng and J. Liu, "Investigations on Three-Dimensional Coupled Flow of Secondary Air System and Main Flow Passages in a Micro Gas Turbine," in *ASME Turbo Expo*, Düsseldorf, 2014.
- [14] L. Bozzi and E. D'angelo, "Numerical and Experimental Investigation of Secondary Flows and Influence of Air System Design on Heavy-Duty Gas Turbine Performance," in *ASME Turbo Expo*, Copenhagen, 2012.
- [15] P. L. Meitner, "Procedure for Determining 1-D Flow Distributions In Arbitrarily Connected Passages Without the Influence of Pumping," in *ASME Turbo Expo*, Atlanta, 2003.
- [16] M. J. Holland and T. F. Thawke, "Rotor Blade Cooling in High Pressure Turbines," *Journal of Aircraft*, vol. 17, pp. 412-418, 1980.
- [17] L. Torbidoni and J. H. Horlock, "A New Method to Calculate the Coolant Requirements of a High-Temperature Gas Turbine Blade," *J. Turbomach*, vol. 127, pp. 191-199, 2005.

